

Electronic Supplementary Information

ABaSbQ₃ (A = Li, Na; Q = S, Se): diverse arrangement modes of isolated SbQ₃ ligands regulating the magnitudes of birefringences

Ailijiang Abudurusuli,^{ab,‡} Kui Wu,^{a,‡} Abudukadi Tudi,^{ab} Zihua Yang, Shilie Pan^{*a}

^aCAS Key Laboratory of Functional Materials and Devices for Special Environments, Xinjiang Technical Institute of Physics & Chemistry, CAS; Xinjiang Key Laboratory of Electronic Information Materials and Devices, 40-1 South Beijing Road, Urumqi 830011, China.

^bCenter of Materials Science and Optoelectronics Engineering, University of Chinese Academy of Sciences, Beijing 100049, China.

[‡] Ailijiang Abudurusuli and Kui Wu contributed equally.

To whom correspondence should be addressed :

E-mail: span@ms.xjb.ac.cn (Shilie Pan).

CONTENTS

- 1. Synthesis of Title Compounds**
- 2. Structural Refinement and Crystal Data**
- 3. Property Characterization**
- 4. Figures and Tables**
- 5. References**

EXPERIMENTAL SECTION

Reagents and Synthesis. All the raw reagents (Li, Na, Ba, BaS, Sb, S, Se) with purities higher than 99.99% were commercially purchased by Aladdin Industrial Inc. and were stored in a dry Ar-filled glovebox with limited oxygen and moisture levels below 0.1 ppm. Since the Li/Na/Ba metals easily react with the oxygen in the air, the entire weighing processes were carried out in the glovebox.

Synthesis of NaBaSbS₃ and LiBaSbS₃. The target compounds were prepared through conventional solid state reaction method with the following steps. (1) The starting materials Li/Na, BaS, Sb, and S with molar ratio of 1:1:1:2 were weighed and loaded into graphite crucible, then were put into fused silica tubes (length 20 cm, diameter 1 cm). (2) The silica tubes were sealed with methane-oxygen flame under a high vacuum of 10⁻³ Pa. (3) The sealed tubes were moved into computer-controlled furnaces and heating program setting to 900 °C in 60 h, left for 100 h to ensure the mixture completely melted, after that the temperature was cooled to 300 °C at a rate of 3 °C/h, the furnace was turned off. (4) The obtained products were repeatedly washed with the N, N-dimethylformamide (DMF) for removing the other byproducts. Finally the target compounds with the red color were found and they were stable in air.

Synthesis of NaBaSbSe₃, LiBaSbSe₃. The synthesis processes of selenides were similar to the sulfides, except the different molar ratio of Na/Li:Ba:Sb:Se = 1:1:1:3, and the temperature was set to the same temperature as sulfides. After the reaction, the obtained products were rinsed with DMF to remove byproducts, and final air stable red color crystals were obtained.

Single-Crystal X-ray Diffraction (XRD). High-quality single crystals were selected under an optical microscope for collecting the X-ray diffraction data. A Bruker SMART APEX II CCD single crystal X-ray diffractometer using graphite-monochromatized molybdenum K α radiation ($\lambda = 0.71073 \text{ \AA}$) was performed to measure crystal data at room temperature. The collected data were corrected for Lorentz and polarization factors, and multi-scan absorption corrections were carried out by XPREP program.^[1] After refining several times by using SHELXTL program

package,^[2] the reasonable R values were obtained, and the formula of compounds were determined to be $ABaSbQ_3$ ($A = \text{Li, Na}$; $Q = \text{S, Se}$). The final structures were also checked with PLATON, and no other higher symmetry elements were found.^[3] Crystallographic data and structural refinement details are presented in Table S1, and atomic coordinates as well as selected bond distances and angles are displayed in Tables S2, Supporting Information (ESI).

Powder X-ray Diffraction. Bruker D2 PHASER diffractometer with Cu $K\alpha$ radiation ($\lambda = 1.5418 \text{ \AA}$) was applied for measuring the XRD data of powder samples of title compounds at a room temperature. The 2θ range was $10\text{--}70^\circ$ with a step size of 0.02° and a fixed counting time of 1 s per step. From Fig. S1, it can be seen that the experimental powder XRD patterns of the samples are in good agreement with the calculated (no obvious by-products) patterns derived from CIF data, which further demonstrate the accuracy of this work.

UV-Vis-NIR Diffuse Reflectance Spectroscopy. The optical diffuse-reflectance spectra of the title compounds were measured at room temperature using SolidSpec-3700DUV spectrophotometer in the wavelength range from 200 to 2600 nm. The collection data were converted to absorbance using the Kubelka–Munk function to figure out the band gap.

Raman Spectroscopy. The high quality ground crystals were put on a transparent glass slide, and then a LABRAM HR Evolution spectrometer equipped with a CCD detector by a 532 nm radiation was applied to investigate the Raman spectra in the $4000\text{--}100 \text{ cm}^{-1}$ region ($2.5\text{--}100 \text{ }\mu\text{m}$).

Theoretical Calculations. To better explain the relationship between the structure-property, the electronic structures and optical properties were calculated based on density functional theory (DFT).^[4] The Perdew–Burke–Ernzerhof (PBE) function was chosen to calculate the exchange–correlation potential, with an energy cutoff of 770.0 eV under the generalized gradient approximation (GGA).^[5] The valence electrons were set as $1s^2 2s^1$ configuration for Li, $2s^2 2p^6 3s^1$ for Na, $5s^2 5p^6 6s^2$ for Ba, $3s^2 3p^4$ for S, $4s^2 4p^4$ for Se and $5s^2 5p^3$ for Sb. To acquire energy convergence, the ion-electron interactions were modeled by the norm-conserving pseudopotential (NCP)

for all elements. The kinetic energy cutoff of was 770 eV within the NCP was employed throughout the calculations and the Monk-horst-Pack k-point meshes of NaBaSbQ₃ (8 × 3 × 6) and LiBaSbQ₃ (5 × 5 × 6) in the primitive cell were chosen to achieve a well converged electronic structure and optical properties.^[6] Since the discontinuity of exchange correlation energy, the experimental value is often larger than that of calculated band gap.

On the basis of the electronic structures, the imaginary part of dielectric function ϵ_2 can be calculated, and its real part is determined by the Kramers–Kronig transform, from which the refractive indices (and the birefringence Δn) were obtained.^[8] The calculation of optical properties was scissor-corrected by the difference between the calculated and measured energy gaps. A real-space atom-cutting technique was applied to analyze the contribution of an ion (or ionic group) to the first-order susceptibility $\chi^{(1)}$.^[9] The contribution of ion A to the first-order polarizabilities is denoted as $\chi^{(1)}(A)$, it can be obtained by cutting all ions except A from the original wave functions $\chi^{(1)}(A) = \chi^{(1)}(\text{all ions except A are cut})$.

Table S1 Crystal Data and Structure Refinement for ABaSbQ₃ (A = Na, Li; Q = S, Se).

Empirical formula	NaBaSbS ₃	NaBaSbSe ₃	LiBaSbS ₃	LiBaSbSe ₃
Formula weight	378.26	518.96	724.42	502.91
Temperature	293(2) K	293(2) K	293(2) K	293(2) K
Wavelength	0.71073 Å	0.71073 Å	0.71073 Å	0.71073 Å
Crystal system,	Monoclinic	Monoclinic	Orthorhombic	Orthorhombic
Space group	<i>P2₁/c</i>	<i>P2₁/c</i>	<i>Pbam</i>	<i>Pbam</i>
Unit cell dimensions	a = 6.0668(16) Å	a = 6.291(11) Å	a = 11.673(3) Å	a = 12.117(4) Å
	b = 14.232(4) Å	b = 14.80(2) Å	b = 12.166(3) Å	b = 12.644(5) Å
	c = 7.778(2) Å	c = 8.072(13) Å	c = 8.780(2) Å	c = 9.102(3) Å
	β = 105.58°	β = 105.484°		
Volume (Å ³)	646.90(62)	724.28(430)	1246.9(5)	1394.5(9)
Z, Calculated density	4, 3.884 Mg/m ³	4, 4.760 Mg/m ³	8, 3.859 Mg/m ³	8, 4.791 Mg/m ³
Absorption coefficient	11.119 mm ⁻¹	24.152 mm ⁻¹	11.464 mm ⁻¹	25.014 mm ⁻¹
F(000)	664.0	880.0	1264	1696
Crystal size (mm ³)	0.150 × 0.112 × 0.095	0.174 × 0.131 × 0.089	0.156 × 0.124 × 0.094	0.186 × 0.112 × 0.098
Completeness to theta	99.8%	98.7%	99.8%	99.8%
Goodness-of-fit on F^2	1.192	0.955	1.032	1.045
Final R indices	$R_1 = 0.0200,$	$R_1 = 0.0311,$	$R_1 = 0.0192,$	$R_1 = 0.0198,$
$[(F_o^2 > 2\sigma(F_o^2))]^{[a]}$	$wR_2 = 0.0414$	$wR_2 = 0.0542$	$wR_2 = 0.0373$	$wR_2 = 0.0390$
R indices (all data) ^[a]	$R_1 = 0.0226,$	$R_1 = 0.0415,$	$R_1 = 0.0240,$	$R_1 = 0.0260,$
	$wR_2 = 0.0539$	$wR_2 = 0.0569$	$wR_2 = 0.0392$	$wR_2 = 0.0415$
Extinction coefficient	0.0054(3)	0.00089(10)	0.00119(5)	0.00112(4)
Largest diff. peak and hole (e. Å ⁻³)	1.091 and -1.074	1.278 and -1.275	0.798 and -0.879	0.843 and -0.947

$$^{[a]}R_1 = F_o - F_c / F_o \text{ and } wR_2 = [w(F_o^2 - F_c^2)^2 / wF_o^4]^{1/2} \text{ for } F_o^2 > 2\sigma(F_o^2)$$

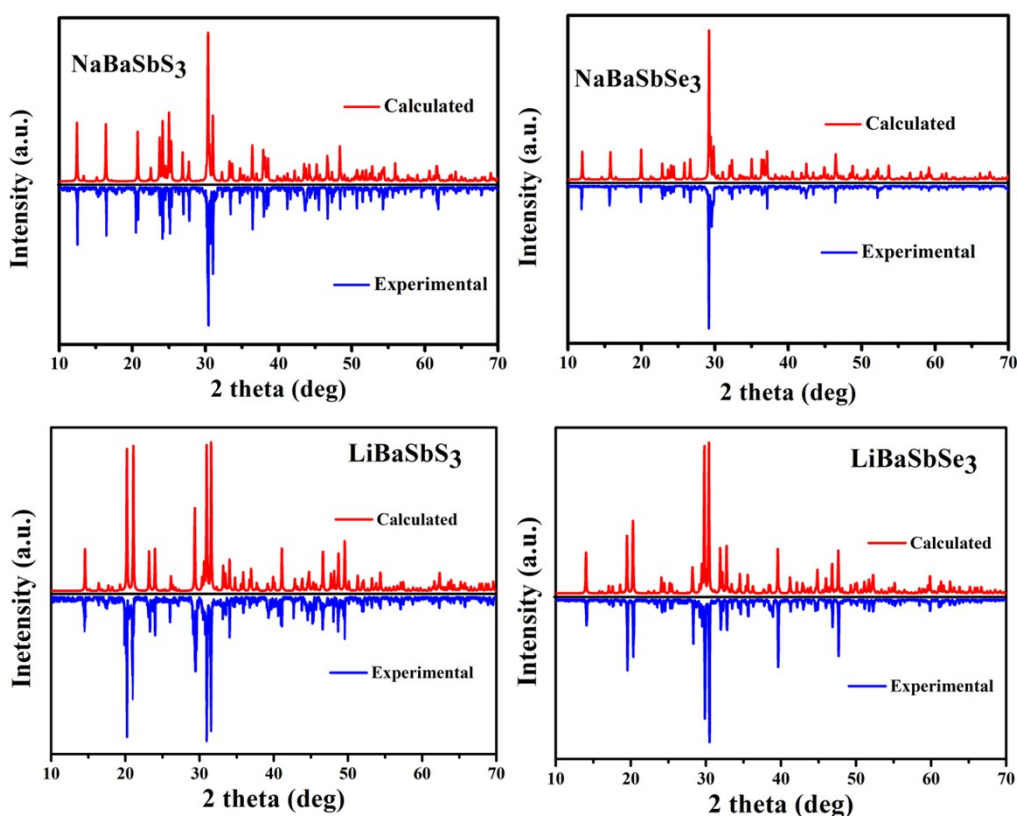


Fig. S1 Powder XRD patterns for title compounds.

Table S2. Selected bond lengths and bond angles for title compounds.

Compounds	SbQ ₄ : Sb-Q (Å)	M ^{III} Q ₄ : Q-M-Q (deg)	AQ _n : A-Q (Å)	MQ ₇ : M-Q (Å)
NaBaSbS ₃	Sb-S: 2.40, 2.43×2	S-Sb-S: 102.1, 97.1, 98.9	Na-S: 2.77, 2.84, 3.03, 3.06	Ba-S: 3.13, 3.17, 3.24, 3.26, 3.29
NaBaSbSe ₃	Sb-Se: 2.57×2, 2.55	Se-Sb-Se: 97.1, 102.1, 98.9	Na-Se: 2.88, 3.94, 3.05, 3.14, 3.17	Ba-Se: 3.27×2, 3.30, 3.38, 3.41
LiBaSbS ₃	Sb1-S: 2.42×2, 2.43 Sb2-S: 2.431×3	S-Sb1-S: 95.1×3, S-Sb2-S: 94.4×2, 98.3	Li-S: 2.36, 2.38, 2.51, 2.58	Ba-S: 3.39×4, 3.21×4, 3.42×2
LiBaSbSe ₃	Sb1-Se: 2.56×2, 2.55 Sb2-Se: 2.56×3	Se-Sb1-Se: 95.1×3 S-Sb2-Se: 94.1×2, 97.6	Li-Se: 2.45, 2.47, 2.63, 2.65	Ba-Se: 3.24×4, 3.45×4, 3.48×2

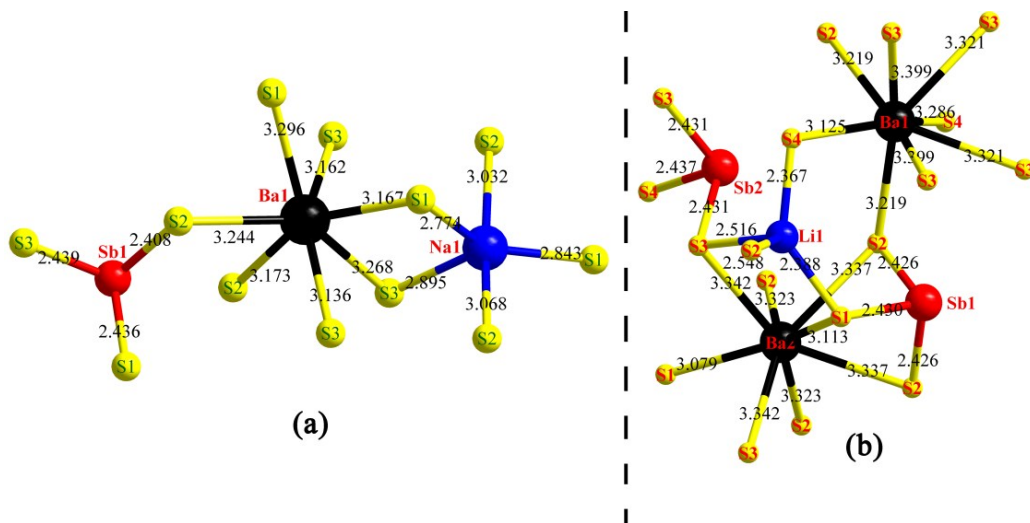


Fig. S2 Selected bond lengths and coordination environments (a) NaBaSbS₃, (b) LiBaSbS₃.

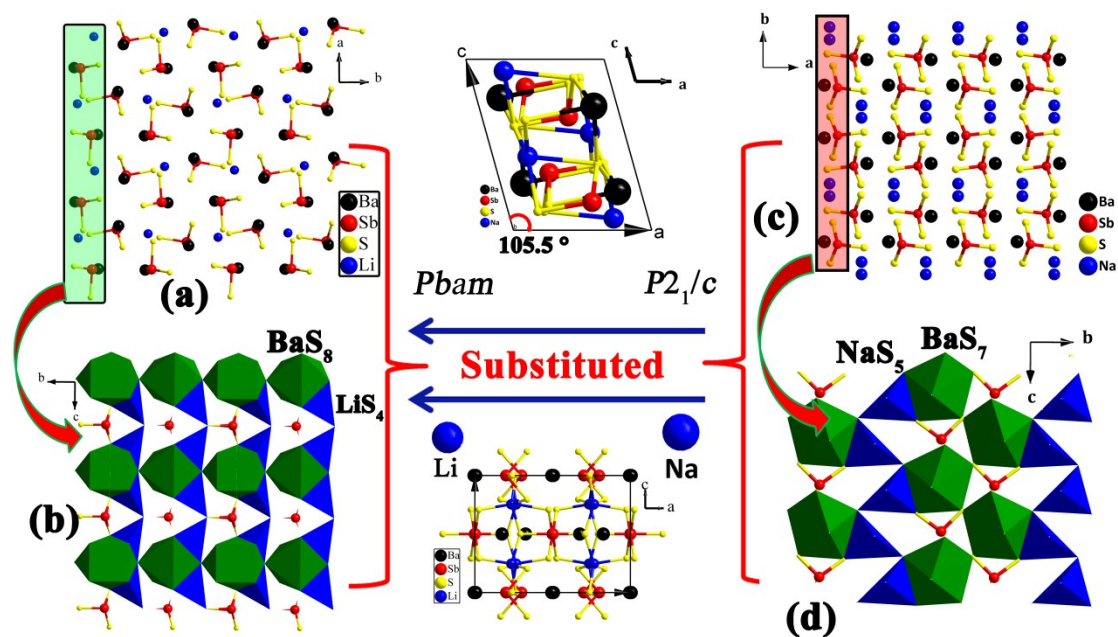


Fig. S3 Structural comparison among title compounds. (a) Atomic distribution in LiBaSbS₃. (b) Layers composed by the LiS₄ tetrahedra and the BaS₈ polyhedra connecting with each other by sharing faces. (c) Atomic distribution in NaBaSbS₃. (d) Layers composed by the NaS₅ and BaS₇ polyhedra linking with each other via sharing edges.

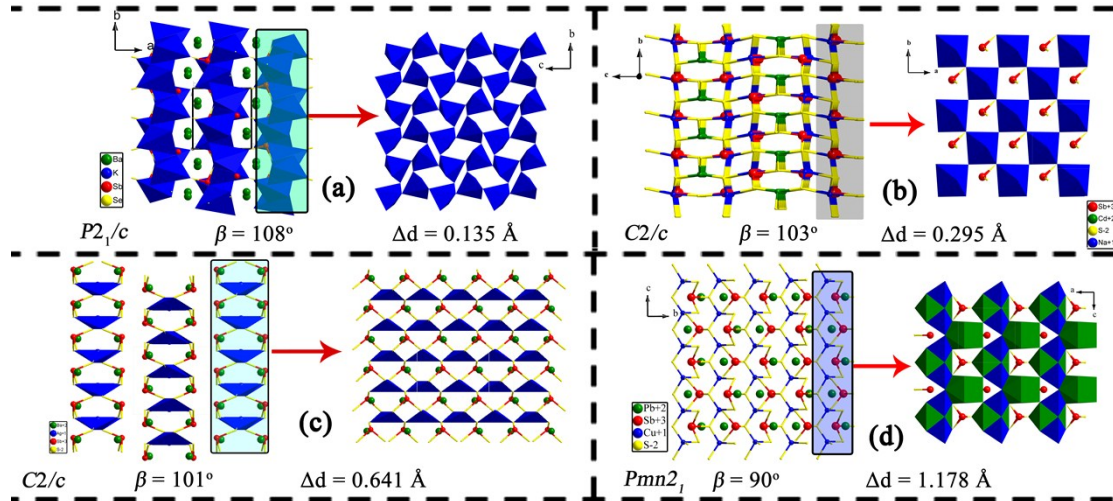


Fig. S4 (a) The irregular KS_5 polyhedra are hold together by sharing corners to form the KS_5 layers, and the BaS_7 poyhedra are distributed in the KS_5 interlayers to build 3D structure; (b) The compounds NaCdSbS_3 , KHgSbS_3 are isostructural ($C2/c$), and in their structures, the isolated trigonal-pyramidal SbS_3 and the NaS_6/KS_6 polyhedra connect with each other to form layers, which are further linked together by the $\text{CdS}_4/\text{HgS}_4$ tetrahedra to build final 3D structure; (c) The major structures of AgBaSbS_3 are composed of the AgS_4 chains interconnecting by isolated SbQ_3 pyramids and the BaQ_7 polyhedra to construct the final 3D framework; (d) CuPbSbS_3 crystallizes in the noncentrosymmetric $Pmn2_1$ space group of orthorhombic system, and its structure contains isolated infinite CuS_4 chains, isolated SbS_3 units and PbS_n ($n = 7, 8$) polyhedra, which are interlinked with each other to construct the 3D network.

Table S3. The space group, bonds length differences Δd , tilting angles β and calculated birefringence values for the compounds in the A-M^{II}-Sb-Q₃ system.

Compounds	Space group	β (deg)	$\Delta d = L_{M^{II}-Q} - L_{A-Q}$ (Å)	Calculated Δn	Crystal system	Ref.
KHgSbS ₃	<i>C2/c</i>	105.7	0.572	0.14	Monoclinic system	9
AgBaSbS ₃	<i>C2/c</i>	101.7	0.641	0.15		10
NaCdSbS ₃	<i>C2/c</i>	103.5	0.295	0.14		11
AgPbSbS ₃	<i>P2₁/c</i>	92.25	0.647	0.25		12
KBaSbSe ₃	<i>P2₁/c</i>	108.25	0.135	0.11		13
NaBaSbS₃	<i>P2₁/c</i>	105.5	0.401	0.22		This work
NaBaSbSe₃	<i>P2₁/c</i>	105.5	0.274	0.24	This work	
LiBaSbS₃	<i>Pbam</i>	90	0.870	0.03	Orthorhombic system	This work
LiBaSbSe₃	<i>Pbam</i>	90	0.822	0.03		This work
CuBaSbS ₃	<i>Pbam</i>	90	0.932	0.05		14
CuBaSbSe ₃	<i>Pbam</i>	90	0.978	0.04		14
CuPbSbS ₃	<i>Pmn2₁</i>	90	1.178	0.08		15

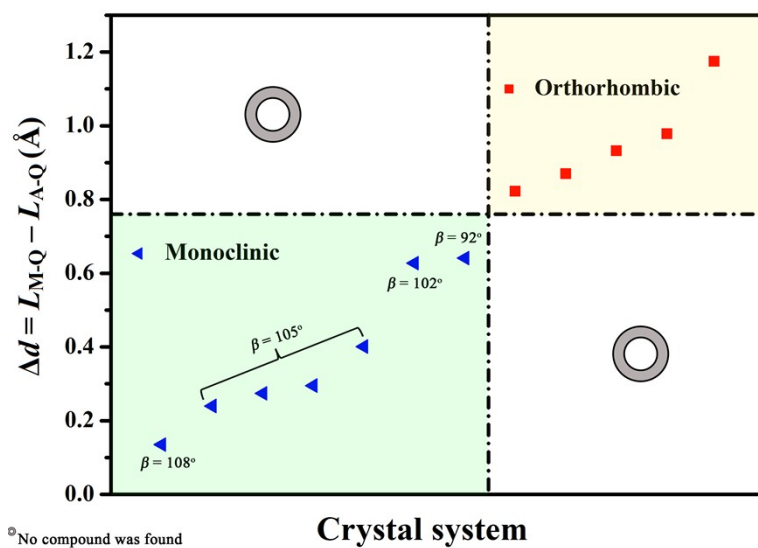


Fig. S5 Summary of bond length differences Δd , tilting angles β , and crystal system in AM^{II}SbQ₃ compounds.

Table S4. Summary of the maximum bond length differences ($\Delta d = L_{M^{II-Q}} - L_{A-Q}$) for other Sb-based system.

Chalcogenides					
Compound	Space group	SbQ _n	$\Delta d = L_{M^{II-Q}} - L_{A-Q}$ (Å)	Sb valence state	Crystal system
CuK ₂ SbS ₃	<i>P2₁/c</i>	SbS ₃	1.052	+3	Monoclinic
CuNa ₂ SbS ₃	<i>P2₁/c</i>	SbS ₃	0.668	+3	
Rb ₂ Cu ₂ Sb ₂ S ₅	<i>P2₁/c</i>	SbS ₃	1.225	+3	
CsCuSb ₂ S ₄	<i>C2/c</i>	SbS ₄	1.105	+3	
AgRb ₂ SbS ₄	<i>P2₁/c</i>	SbS ₄	0.687	+3	
CuRbSb ₂ S ₄	<i>C2/c</i>	SbS ₄	1.068	+3	
AgCsSb ₄ S ₇	<i>C2/c</i>	SbS ₃	0.538	+3	
Ag ₄ MnSb ₂ S ₆	<i>P2₁/c</i>	SbS ₃	0.103	+3	
CuPb ₁₃ Sb ₇ S ₂₄	<i>Pnma</i>	SbS ₃	0.847	+3	Orthorhombic
Ag ₃ K ₂ Sb ₃ S ₇	<i>Cmc2₁</i>	SbS ₃	0.893	+3	
AgPbSb ₃ S ₆	<i>Cmcm</i>	SbS ₅	0.893	+3	
AgK ₂ SbS ₄	<i>Pnn2</i>	SbS ₄	1.115	+5	
Ag ₉ K ₃ Sb ₄ S ₁₂	<i>I4/m</i>	SbS ₃	0.309	+3	Tetragonal
Ag ₂ KSbS ₄	<i>I4₂m</i>	SbS ₄	0.873	+5	
Cu ₂ KSbS ₃	<i>P1</i>	SbS ₃	1.242	+3	Triclinic
Ag ₂ KSbS ₃	<i>P1</i>	SbS ₃	0.938	+3	
Oxides					
LiSr ₃ SbO ₆	<i>R3c</i>	SbO ₆	0.345	+5	Trigonal
NaBa ₃ SbO ₆	<i>R3c</i>	SbO ₆	0.57	+5	
NaSr ₃ SbO ₆	<i>R3c</i>	SbO ₆	0.225	+5	
Ag ₃ Co ₂ SbO ₆	<i>P3₁12</i>	SbO ₆	0.201	+5	
Ag ₅ HgSbO ₆	<i>P3₁c</i>	SbO ₆	0.098	+5	
AgHg ₃ SbO ₆	<i>R3c</i>	SbO ₆	0.498	+5	
Cu ₃ Mg ₂ SbO ₆	<i>R3</i>	SbO ₆	0.255	+5	
Cu ₂ Li ₃ SbO ₆	<i>C2/c</i>	SbO ₆	0.004	+5	Monoclinic
Li ₃ Zn ₂ SbO ₆	<i>C2/m</i>	SbO ₆	0.014	+5	
Co ₂ Cu ₃ SbO ₆	<i>C2/c</i>	SbO ₆	0.266	+5	

$\text{Cu}_2\text{Na}_3\text{SbO}_6$	$C2/m$	SbO_6	0.217	+5	Cubic
$\text{NaSr}_4\text{Sb}_3\text{O}_{12}$	$P2_1/c$	SbO_6	0.521	+5	
$\text{K}_2\text{NaSb}_3\text{O}_9$	$Pn\bar{3}$	SbO_3	0.092	+5	
$\text{NaBa}_4\text{Sb}_3\text{O}_{12}$	$Im\bar{3}m$	SbO_6	0.685	+5	
$\text{CuBa}_3\text{Sb}_2\text{O}_9$	$P6_3/mmc$	SbO_6	1.049	+5	Hexagonal
KZn_4SbO_7	$P6_3mc$	SbO_6	1.093	+5	
CuLiSbO_4	$Cmc2_1$	SbO_6	0.039	+5	Orthorhombic
$\text{CuLi}_3\text{SbO}_5$	$P\bar{1}$	SbO_6	0.133	+5	Triclinic

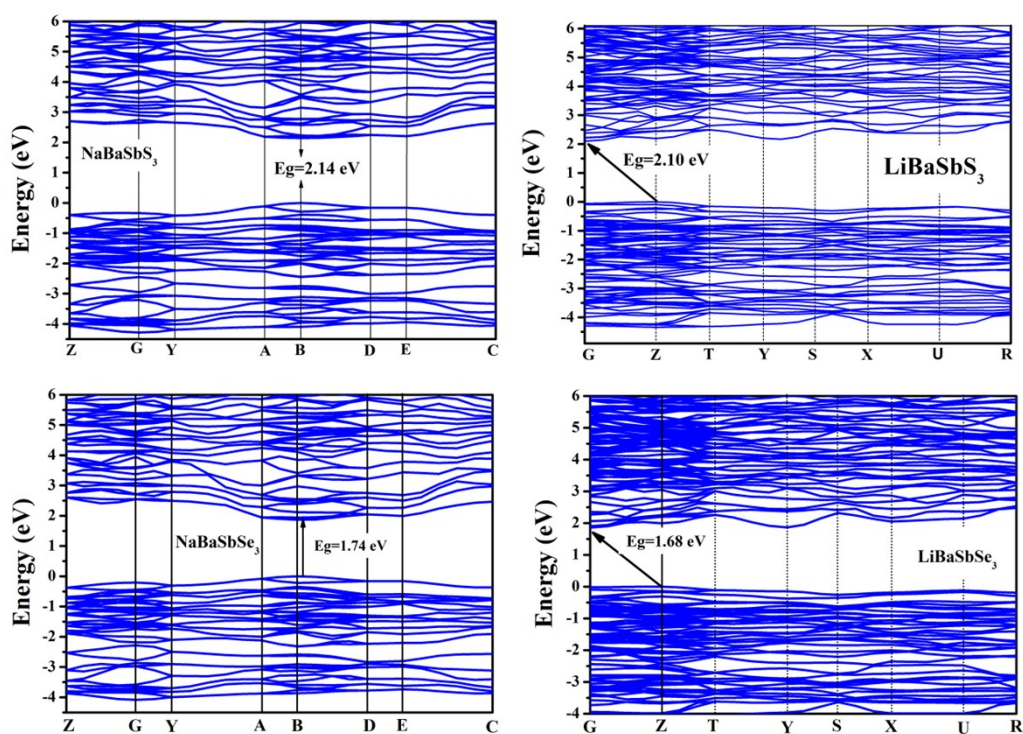


Fig. S6 Calculated band structures for title compounds.

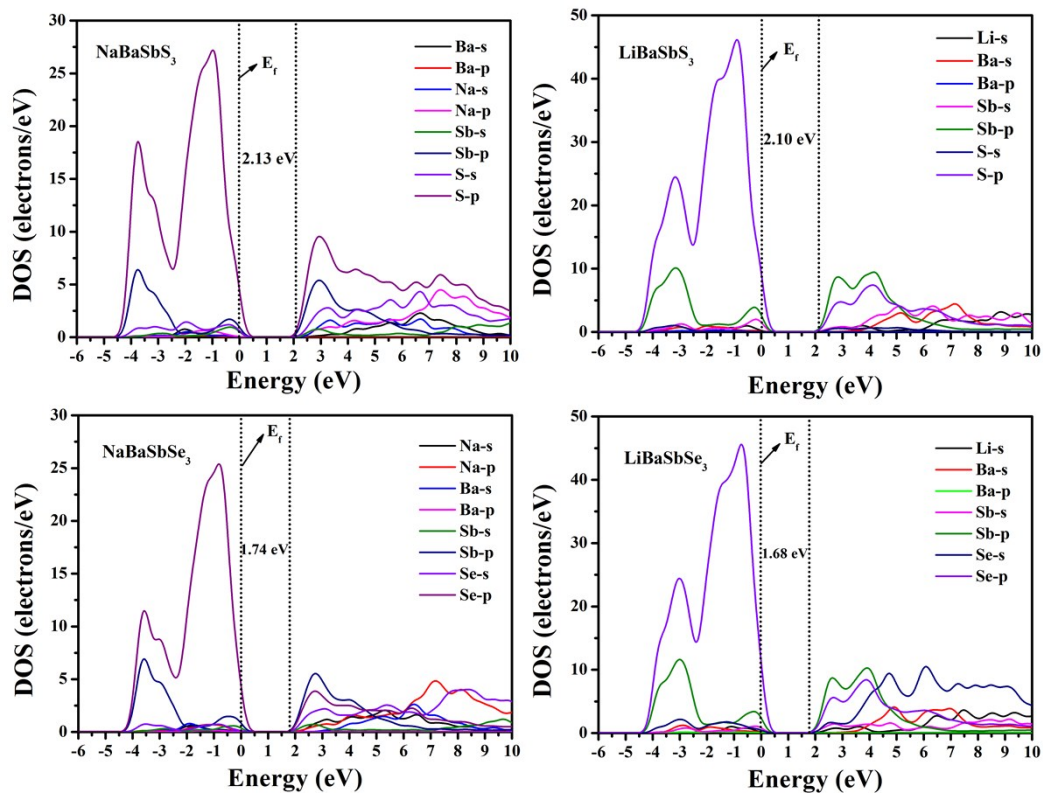


Fig. S7 The partial density states (PDOS) for title compounds.

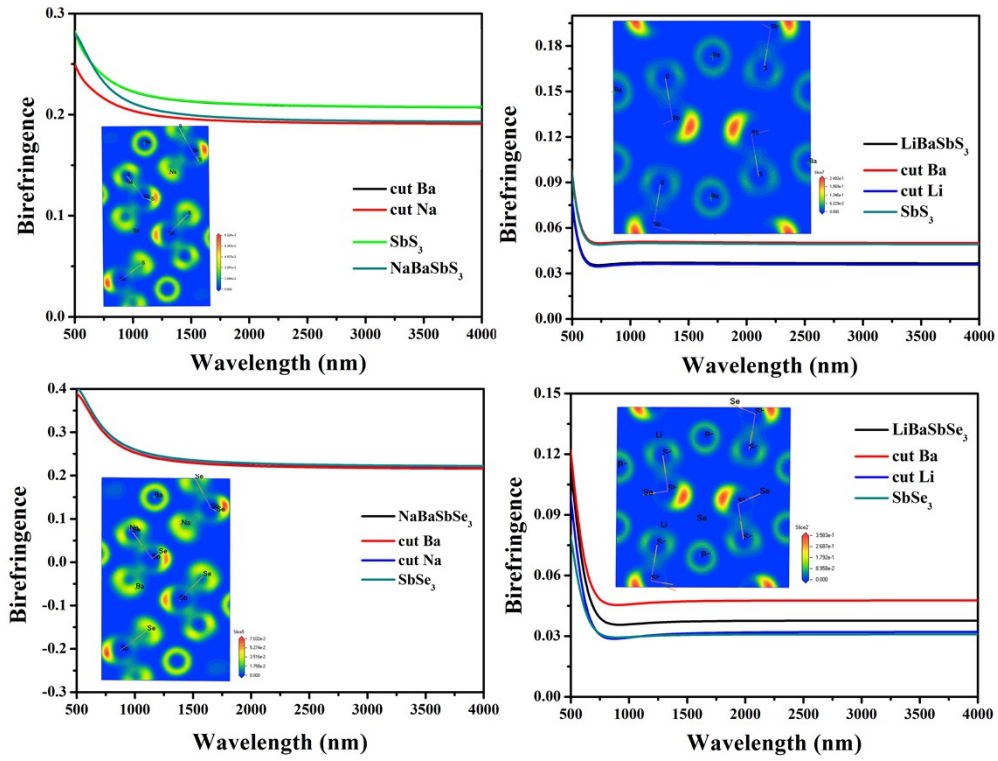


Fig. S8 The contribution of different groups to the birefringence and ELF for title compounds.

Table S5. Birefringence of different groups for title compounds.

Different groups	Birefringence (1064 nm)	Birefringence (532 nm)
NaBaSbS₃	0.22	0.30
SbS ₃	0.24	0.31
Cut Na	0.22	0.29
Cut Ba	0.24	0.32
NaBaSbSe₃	0.24	0.38
SbSe ₃	0.25	0.39
Cut Na	0.24	0.39
Cut Ba	0.25	0.38
LiBaSbS₃	0.03	0.06
SbS ₃	0.05	0.07
Cut Na	0.03	0.06
Cut Ba	0.05	0.08
LiBaSbSe₃	0.03	0.09
SbSe ₃	0.03	0.08
Cut Na	0.03	0.06
Cut Ba	0.04	0.10

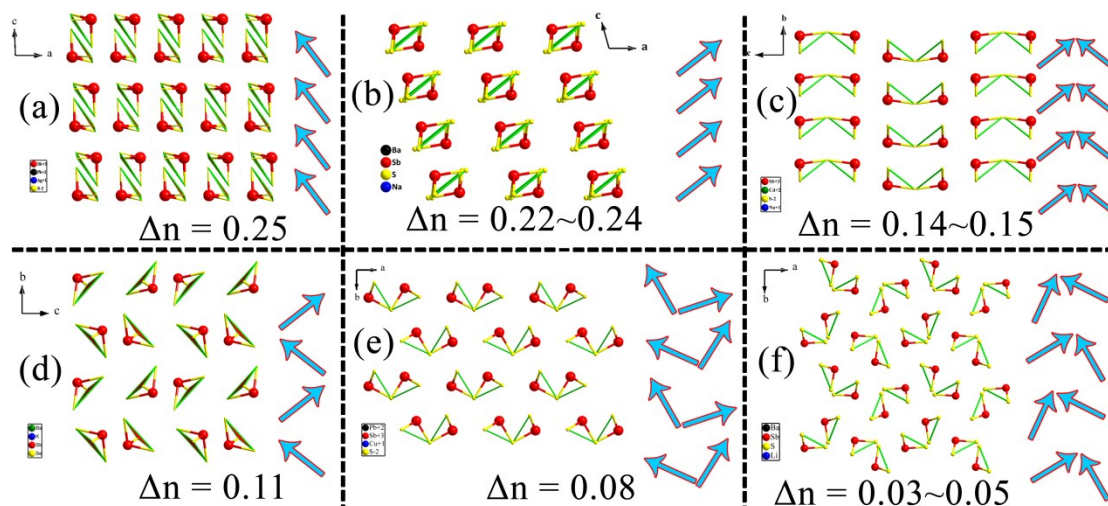


Fig. S9 Arrangements of the SbQ_3 groups in the $\text{A-M}^{\text{II}}\text{-Sb-Q}_3$ system; (a) AgPbSbS_3 ; (b) NaBaSbQ_3 ; (c) KHgSbS_3 , AgBaSbS_3 , NaCdSbS_3 ; (d) KBaSbSe_3 ; (e) CuPbSbS_3 ; (f) CuBaSbQ_3 , LiBaSbQ_3 .

References

- [1] G. M. Sheldrick, *SHELXTL*, version 6.14; Bruker Analytical X-ray Instruments, Inc.: Madison, WI, 2003.
- [2] *SAINTE*, version 7.60A; Bruker Analytical X-ray Instruments, Inc.: Madison, WI, 2008.
- [3] A. L. Spek, *J. Appl. Crystallogr.*, 2003, **36**, 7.
- [4] S. J. Clark, M. D. Segall, C. J. Pickard, P. J. Hasnip, M. J. Probert, K. Refson and M. C. Payne, *Z. Kristallogr.*, 2005, **220**, 567.
- [5] J. P. Perdew, K. Burke and M. Ernzerhof, *Phys. Rev. Lett.*, 1996, **77**, 3865.
- [6] A. M. Rappe, K. M. Rabe, E. Kaxiras and J. D. Joannopoulos, *Phys. Rev. B*, 1990, **41**, 1227.
- [7] L. Kang, S. Y. Luo, H. W. Huang, N. Ye, Z. S. Lin, J. G. Qin, C. T. Chen, *J. Phys. Chem. C*, 2013, **117**, 25684.
- [8] J. Lin, M. H. Lee, Z. P. Liu, C. T. Chen, C. J. Pickard, *Phys. Rev. B*, 1999, **60**, 13380.
- [9] M. Imafuku, I. Nakai, K. Nagashima, *Mater. Res. Bull.*, 1986, **21**, 493.
- [10] C. Liu, Y. Y. Shen, P. P. Hou, M. J. Zhi, C. M. Zhou, W. X. Chai, J. W. Cheng, Y. Liu, *Inorg. Chem.*, 2015, **54**, 8931.
- [11] Y. D. Wu, W. Bensch, *J. Alloys Compd.*, 2012, **511**, 35.
- [12] A. Galdámez, F. López-Vergara, P. Barahona, V. Manríquez, R. E. Ávila, *J. Solid State Electr.*, 2012, **16**, 697.
- [13] W. L. Yin, K. Feng, L. Kang, B. Kang, J. G. Deng, Z. S. Lin, Y. C. Wu, *J. Alloys Compd.*, 2014, **617**, 287.
- [14] C. Liu, P. P. Hou, W. X. Chai, J. W. Tian, X. R. Zheng, Y. Y. Shen, Y. Liu, *J. Alloys Compd.*, 2016, **679**, 420.
- [15] A. Faghaninia, G. Yu, U. Aydemir, M. Wood, W. Chen, G. M. Rignanese, A. Jain, *Phys. Chem. Chem. Phys.*, 2017, **19**, 6743.